C. R. Physique 16 (2015) 51–61

Contents lists available at ScienceDirect

Comptes Rendus Physique

www.sciencedirect.com

Granular physics / Physique des milieux granulaires

Kinetic theory for sheared granular flows

Théorie cinétique des écoulements granulaires cisaillés

Viswanathan Kumaran

Department of Chemical Engineering, Indian Institute of Science, Bangalore 560 012, India

ARTICLE INFO

Article history:
Available online 13 January 2015

Keywords:
Granular kinetic theory
Sheared granular flows
Dense granular flows

Mots-clés :
Théorie cinétique granulaire
Écoulements granulaires cisaillés
Écoulements granulaires denses

ABSTRACT

Rapid granular flows are far-from-equilibrium-driven dissipative systems where the interaction between the particles dissipates energy, and so a continuous supply of energy is required to agitate the particles and facilitate the rearrangement required for the flow. This is in contrast to flows of molecular fluids, which are usually close to equilibrium, where the molecules are agitated by thermal fluctuations. Sheared granular flows form a class of flows where the energy required for agitating the particles in the flowing state is provided by the mean shear. These flows have been studied using the methods of kinetic theory of gases, where the particles are treated in a manner similar to molecules in a molecular gas, and the interactions between particles are treated as instantaneous energy-dissipating binary collisions. The validity of the assumptions underlying kinetic theory, and their applicability to the idealistic case of dilute sheared granular flows are first discussed. The successes and challenges for applying kinetic theory for realistic dense sheared granular flows are then summarised.

RÉSUMÉ

Les écoulements granulaires rapides sont des systèmes forcés hautement dissipatifs hors équilibre, dans lesquels les interactions entre particules dissipent l'énergie, et qui, de ce fait, requièrent un apport énergétique ininterrompu pour agiter les particules et faciliter les réarrangements nécessaires à l'écoulement. Ceci les différencie des écoulements de fluides moléculaires, qui sont en général proches de l'équilibre, et dont les molécules sont agitées par des fluctuations thermiques. Les écoulements granulaires cisaillés constituent une classe dans laquelle l'énergie nécéssaire est fournie par le cisaillement moyen. Ils sont étudiés à l'aide de la théorie cinétique des gaz, dans laquelle les particules sont traitées comme des molécules gazeuses, et où leurs intéractions sont binaires, instantanées et dissipatives. Nous discutons d'abord le bien-fondé de ces hypothèses qui sous-tendent la théorie cinétique et leur emploi dans le cas idéaliste d'un écoulement granulaire dilué. Nous résumons ensuite les succès et les défis attachés à la mise en œuvre de la théorie cinétique dans des écoulements réalistes denses et cisaillés.

E-mail address: kumaran@chemeng.iisc.ernet.in.

http://dx.doi.org/10.1016/j.crhy.2014.11.008
1631-0705/

1. Introduction

The physics of granular flows is a fascinating subject because a range of complex collective behaviour arise from seemingly simple microscopic interactions between the individual grains. The experiments of Faraday [1] on convection rolls in granular heaps was perhaps the first illustration of complex flows generated in granular media. Since then, there have been many studies on complex phenomena such as the formation of convection rolls [2], surface waves [3], patterns, and solitary waves [4]. Most of these complex phenomena can be reproduced in simulations using simple interactions at the grain level [5–7], where the grains are considered as soft or hard spheres. However, we currently lack a theoretical framework for starting from the microscopic particle interaction laws and deriving macroscopic equations. A relatively simpler phenomenon, which currently is not adequately explained on the basis of microscopic interaction laws, is the transition from a static to a flowing state when the angle of inclination of a granular material exceeds a critical value called the angle of repose. While the initiation of flow has been attributed to a 'yield stress' due to the friction between the grains in the static state, it is more difficult to explain the cessation of flow when the angle of inclination decreases below a critical value. In contrast, a horizontal layer of a Newtonian fluid flows even when tilted by an infinitesimal angle. This simple flow cessation phenomenon illustrates the difficulty in arriving at a macroscopic description for granular flows in a manner similar to the Navier–Stokes equations for Newtonian fluids.

For the purposes of the present review, a granular material is defined as one in which the grains interact only when they are in physical contact. Viscous and inertial forces exerted by the interstitial fluid, electrostatic, van der Waals and other forces are neglected. The contact forces between grains are usually modelled by spring-dashpot models, where the surfaces of rigid grains in contact are permitted to overlap, and the resistive force opposing overlap contains a 'spring' component proportional to the overlap distance, and a 'damping' component proportional to the relative velocity between the grains. More sophisticated models track the tangential and the normal displacements of the surfaces in contact, and resistive forces are exerted both tangential and normal to the surfaces in contact, as discussed in Section 2. The crucial difference between grain interactions and molecular interactions in a fluid is that energy is dissipated in the interaction between grains, and so a constant supply of energy is necessary to agitate the grains and sustain the flow. A further simplification is to consider the interactions between grains as instantaneous binary collisions, where energy is dissipated due to the inelastic nature of the collisions. In the instantaneous collision model, there is no intrinsic time scale associated with the period of interactions between particles. Despite this reduction in the dimensionality of the problem, many of the complex features of granular flow can be reproduced in simulations where collisions are considered instantaneous.

One of the defining ideas in the kinetic theory of sheared granular flows has its origins, ironically, in the study of dense liquid suspensions by Bagnold [8,9]. In his experimental studies on the shear and normal stresses in sheared liquid suspensions in a concentric cylinder rheometer, Bagnold identified two regimes. In the macro-viscous regime at relatively low particle concentrations, the stress was found to be proportional to the strain rate. However, at high concentrations in the 'grain-inertia' regime, Bagnold reported that the stresses are proportional to the square of the strain rate. The rationale for this non-linear dependence on the strain rate was based on a collisional argument—the frequency of collisions is proportional to the difference in velocity between two adjacent streamlines which in turn is proportional to the strain rate, while the impulse (momentum transferred per collision) is also proportional to the strain rate. Since the stress (momentum transported per unit area per unit time) is proportional to the product of the impulse and the collision frequency, there results a regime where the 'Bagnold law' is applicable, that is, the stress is proportional to the square of the strain rate.

In a subsequent experimental study of the recreation of Bagnold's experiments, Hunt et al. [10] found that the non-linear dependence of the stress on strain rate may have been an artefact of a secondary flow generated in the apparatus, due to the relatively small ratio of the height of the suspension and the width of the gap between the cylinders. Nevertheless, based on dimensional analysis, a simpler justification can be provided for the Bagnold law for dry granular flows. If we consider a collisional shear flow of a granular material in which the particles interact only through instantaneous collisions, and in the absence of other forces (viscous, electrostatic, van der Waals, etc.), there is no material time scale associated with the granular material, and the only time dimension is the inverse of the strain rate. Therefore, the Bagnold law, that the stress is proportional to the square of the strain rate, is a dimensional necessity. Though simple dimensionless analysis provides a constitutive relation between the stress and the strain rate, it is very difficult to extend this to more complex situations where the strain rate tensor has multiple components that are spatially varying. The purpose of kinetic theory is to start from a microscopic particle contact model, and derive macroscopic mass, momentum and energy conservation equations by statistical techniques. In Section 2, the instantaneous collision model and its applicability for dense granular flows is examined. The kinetic theory framework for dilute granular flows is summarised in Section 3, followed by a discussion of the extension to dense granular flows in Section 4.

2. Particle contact laws and the instantaneous collision assumption

The most commonly used model for particle-level simulations is the spring-dashpot model proposed by Cundall and Strack [11–14]. This model forms the basis of the Discrete Element Method (DEM) simulation procedure [15–18], which is commonly used for simulating dense granular flows. The particles are usually considered spherical, though more complex shapes are simulated by 'sticking' together spheres. There is an inter-particle force only when there is particle overlap, and the resistance to overlap has two components, a 'spring' component proportional to the overlap distance and a 'damping'

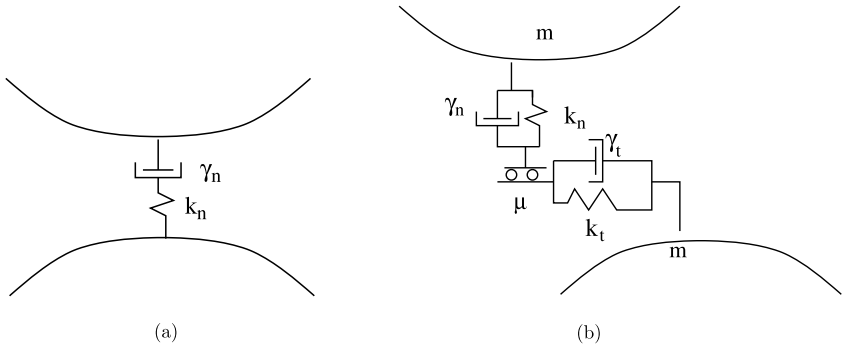

Fig. 1. The contact model for smooth particles (a) and rough particles (b). Here, k_n and k_t are the spring stiffnesses in the normal and tangential to the surfaces of contact, γ_n and γ_t are the damping coefficients normal and tangential to the surfaces of contact, and μ is the friction coefficient.

component proportional to the relative velocity of the particles. In the smooth particle model shown in Fig. 1(a), the forces are only exerted perpendicular to the surfaces at contact. While the linear spring-dashpot model is easy to implement, it does not account for the change in the area of contact, as spheres are pressed against each other. A more realistic model for the contact between spheres is the Hertzian model, where the normal force is proportional to the 3/2 power of the overlap. In the case of rough particles, there are also tangential forces at the contact surfaces, as shown in Fig. 1(b). In the case of frictional particles, the equivalent of a yield criterion is used for particles in contact, with a friction constant μ.

The spring stiffnesses can be related to the Young modulus E of the particles just based on dimensional analysis. The linear spring stiffness, which has dimensions of force per unit distance, has to be proportional to (Ed) times a function of the Poisson ratio, while the Hertzian spring constant has to be proportional to $(Ed^{1/2})$ times a function of the Poisson ratio (ν). An exact result for the Hertzian spring stiffness, $(Ed^{1/2}/3(1-\nu^2))$, was obtained by Mindlin and Deresiewicz [19]. Experiments have been performed on sand grains [20,21] to test the validity of the contact laws used in simulations. In the experiments, the sand particles are mounted on pins and pressed against each other. The displacement and the normal resistive force are measured in order to determine the normal spring stiffness. The experiments indicate that the contact law is linear for rough sand particles due to the compression of asperities, and the spring stiffness is in the range $0.2–2 \times 10^6$ N/m. The contact dynamics is well approximated by the Hertz law for smooth sand grains, though the spring constant is somewhat lower than that predicted using the bulk Young's modulus for the sand material.

The instantaneous collision model is used when the period of interaction is smaller than the time between interactions. In the case of smooth particles, the velocity along the plane tangent to the surfaces at contact remains unchanged, while the post-collisional velocity perpendicular to the surfaces at contact is $-e_n$ times the pre-collisional velocity, where e_n is the normal coefficient of restitution. In the rough particle model, the post-collisional component of the velocity in the plane tangential to the surfaces of contact is $-e_t$ times its pre-collisional value, where e_t is the tangential coefficient of restitution. A formidable calculation by Pidduck [22] based on the molecular model of Bryan [23] has shown that energy is preserved for $e_n = 1$ and $e_t = -1$ (smooth inelastic particles) and for $e_n = 1$ and $e_t = 1$ (rough inelastic particles).

The validity of the instantaneous collision model has been examined in elegant experiments by Foerster et al. [24]. The authors found that collisions can be divided into two types. Head-on collisions are of the sticking type, accurately described by a tangential coefficient of restitution, while grazing collisions are of the sliding type where the tangential force at contact is the product of the normal force and the friction coefficient. Collisions were found to be accurately described by three parameters, the normal and tangential coefficients of restitution and a coefficient of friction. Though most kinetic theory calculations use the smooth inelastic particle model, there are a few calculations [25–27] that have employed the rough particle model, as well as more sophisticated models where the collision is smooth or rough depending on the angle between the line joining the particle centres and the relative velocity.

The period of an interaction for sand particles can be estimated as follows. In the linear spring-dashpot model, the period of a collision, $\pi(2k_n/m - \gamma_n^2/4)^{-1/2}$, is independent of the pre-collisional particle velocities [15]. If we consider particles with density about 1500 kg/m^3 for sand particles or glass beads, and use the linear spring constant of 10^6 N/m as reported by Cole and Peters [20] for rough grains, the time period of a grain interaction is about 2 μs for particles with diameter 1 mm and about 0.1 μs for particles with diameter 100 μm. For the Hertzian contact model, the time period of an interaction does depend on the relative velocity of the particles. However, based on simple dimensional analysis, this can be estimated as $(Ed/m)^{-1/2}$, where E is the Youngs modulus of the particle. If we use the value of $E = 80$ GPa [20], the time period of an interaction for smooth particles is approximately 0.1 μs for particles of diameter 1 mm, and about 0.01 μs for particles of diameter 100 μm. The exceedingly short interaction times suggest that the instantaneous collision approximation is likely to be valid, even for relatively dense flows.

It should be noted that simulations [15,17] typically use much lower spring stiffnesses so that the simulation time step can be made larger. Due to this, the simulation results may predict a much higher co-ordination number (average number of particles in contact with a test particle) in comparison to the real systems. In addition, it is important to note that the spring stiffness calculated should be based on the elasticity modulus of the sand particle itself. Using the speed of sound

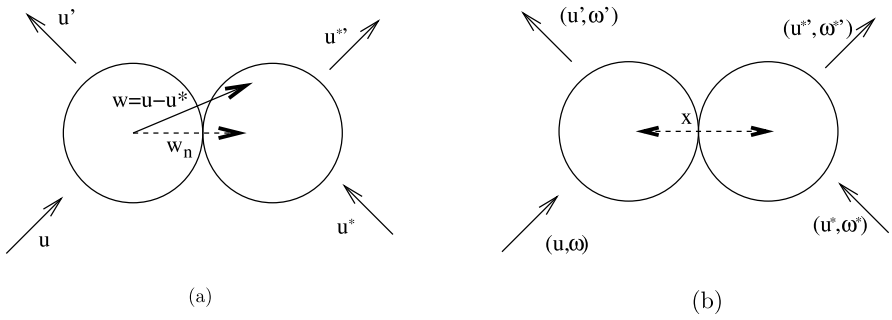

Fig. 2. Collisions between smooth particles (a) and rough particles (b).

through loose sand assemblies [13,14] could lead to unrealistically low values of the spring stiffness, since the speed of sound through loose sand is even less than the speed of sound through air. The effect of variation in spring stiffness on the co-ordination number in dense granular flows were analysed by Reddy and Kumaran [18] for the dense granular flow down an inclined plane [15]. The authors found that the co-ordination number is less than 1 even at very high volume fractions up to about 58% for spring stiffness corresponding to real sand grains as reported by Cole and Peters [20] for both the Hertzian and linear models. The co-ordination number became large only very close to the angle of flow initiation where the volume fraction was greater than 58%. This suggested that the binary collision approximation is valid for higher volume fractions than was suggested by previous simulation studies where unrealistically low values of the stiffness is used.

Distinct from the validity the binary collision approximation is the question of whether the rheology and the constitutive relations change when the spring stiffness is decreased and the system transitions from the binary to the multi-body contact regime. The aforementioned Bagnold relation is a dimensional necessity only when the collision time is much smaller than the time between collisions, so that the there is no material time scale and the only time scale is the inverse of the strain rate. In the multi-body contact regime, the collision time is also expected to influence the dynamics. However, the pioneering simulation results of Silbert et al. [15] showed that the Bagnold law is satisfied even for flows in the multi-body contact regime where the co-ordination number is 3–4. Subsequent computational studies for uniform shear flows [28] and for dense flows down an inclined plane [17,18] have confirmed that there is virtually no change in the stress–strain rate relationship when the spring stiffness of the particles in simulations is decreased by many orders of magnitude, and the flow transitions from a binary collision regime to a multibody contact regime. This intriguing lack of dependence of the rheology on the contact regime is poorly understood, and though there have been reasons suggested [28,18], a lot more work is required to resolve this mystery. However, this also provides significant advantage for modelling, since it indicates that kinetic theory models based on the binary collision approximation do accurately predict the rheology even in the multi-body contact regime.

3. Kinetic theory

In the simplest realisation, a dilute granular material is composed of smooth spherical particles that interact through instantaneous energy-dissipating collisions. Consider a collision between two identical spherical particles of mass m and diameter d, as shown in Fig. 2, where the particles have pre- and post-collisional velocities $(\mathbf{u}, \mathbf{u}^*)$ and post-collisional velocities $(\mathbf{u}', \mathbf{u}^{*'})$. The particle velocities can be expressed in terms of the centre-of-mass velocity $\mathbf{v} = (\mathbf{u} + \mathbf{u}^*)/2$ and the velocity difference $\mathbf{w} = (\mathbf{u} - \mathbf{u}^*)$. Mass is conserved because the particle masses before and after collisions are equal, while momentum is conserved in a collision if the centre-of-mass velocity $\mathbf{v}$ does not change in the collision. In the case of smooth particles, there is an impulse perpendicular to the surfaces of contact along the line joining the centres of the particles, as shown in Fig. 2(a). In the case of rough particles, there are impulse perpendicular and parallel to the surfaces of contact, and there is a change in the angular velocities of the particles at collision as well, from their pre-collisional values of (ω, ω^*) to their post-collisional values of $(\omega', \omega^{*'})$, as shown in Fig. 2(b), consistent with angular momentum conservation.

In kinetic theory, the velocity distribution function is defined such that $n(\mathbf{x}, t) f(\mathbf{x}, \mathbf{u}, t) \mathrm{d}\mathbf{x}\mathrm{d}\mathbf{u}$ is the number of particles in the differential volume d$\mathbf{x}$ about $\mathbf{x}$ in real space and in the differential volume d$\mathbf{u}$ about $\mathbf{u}$ in the velocity co-ordinates. Here, $n(\mathbf{x}, t)$ is the number density of the particles in real space. By definition, the distribution function is normalised,

$$\int_{\mathbf{u}} \mathrm{d}\mathbf{u}\, f(\mathbf{x}, \mathbf{u}, t) = 1 \tag{1}$$

The moments of the distribution function are related to the macroscopic properties of the fluid, the mass, momentum and energy density.

$$\int_{\mathbf{u}} \mathrm{d}\mathbf{u}\, mn(\mathbf{x},t) f(\mathbf{x},\mathbf{u},t) = \rho(\mathbf{x})$$

$$\int_{\mathbf{u}} \mathrm{d}\mathbf{u}\, m\mathbf{u} n(\mathbf{x},t) f(\mathbf{x},\mathbf{u},t) = \rho(\mathbf{x})\mathbf{U}(\mathbf{x})$$

$$\int_{\mathbf{u}} \mathrm{d}\mathbf{u}\left(\frac{m(\mathbf{u}-\mathbf{U})^2}{2}\right) n(\mathbf{x},t) f(\mathbf{x},\mathbf{u},t) = nC_v T \tag{2}$$

where $\rho(\mathbf{x})$ is the local density, $\mathbf{U}(\mathbf{x})$ is the local fluid mean velocity, and T is the temperature in units of energy, and C_v is the specific heat. It is important to note, here, that T is the 'granular temperature' defined on the basis of the fluctuating velocity of the grains, and not the thermodynamic temperature. Physically, $C_v T$ is just the average fluctuating energy per particle. The temperature T is usually written with units of energy, and the specific heat C_v is just a dimensionless constant, which is one half of the number of degrees of freedom, and so the definition in Eq. (2) does not have the Boltzmann constant as a prefactor. The expression for the temperature in Eq. (2) is valid only for smooth particles with translational degrees of freedom, for which $C_v = (3/2)$. In the case of rough particles with rotational degrees of freedom, the distribution function is now a function of the translational and rotational velocities, and the definition of the temperature is,

$$\int_{\mathbf{u}} \mathrm{d}\mathbf{u} \int_{\omega} \mathrm{d}\omega \left(\frac{m(\mathbf{u}-\mathbf{U})^2}{2} + \frac{I(\omega-\Omega)^2}{2}\right) n(\mathbf{x},t) f(\mathbf{x},\mathbf{u},\omega,t) = nC_v T \tag{3}$$

where I is the moment of inertia, ω is the particle angular velocity, Ω is the mean angular velocity of the particles, and the specific heat C_v is 3 for particles with three translational and three rotational degrees of freedom. The distribution function in Eq. (3) is defined such that $n(\mathbf{x},t) f(\mathbf{x},\mathbf{u},\omega,t)\mathrm{d}\mathbf{x}\mathrm{d}\mathbf{u}\mathrm{d}\omega$ is the number of particles in the differential volume $\mathrm{d}\mathbf{x}$ about $\mathbf{x}$ in real space, in the differential volume $\mathrm{d}\mathbf{u}$ about $\mathbf{u}$ in the velocity co-ordinates and in the differential volume $\mathrm{d}\omega$ about ω in the angular velocity co-ordinates. The following description will be restricted to smooth particles for simplicity, but the extension to rough particles is straightforward.

The Enskog equation, which is the conservation equation for the distribution function, can be written as

$$\frac{\partial(nf)}{\partial t} + u_j \frac{\partial(nf)}{\partial x_j} + a_j \frac{\partial(nf)}{\partial u_j} = \frac{\partial_{\mathrm{c}}(nf)}{\partial t} \tag{4}$$

where n is the number density of the particles, $\mathbf{u}$ is the particle velocity and $\mathbf{a}$ is the acceleration of the particles. Here, the indicial notation is used where the components of vectors and tensors are denoted by subscripts $i, j, k, \ldots$, each of which runs from 1 to 3 in three dimensions, the number of subscripts appearing once provides the order of the tensor and a subscript repeated two times is a dot product. The gradients in real space are denoted $(\partial/\partial x_i)$, while the gradients in the velocity co-ordinates are written as $(\partial/\partial u_i)$. The collision integral on the right side of the above equation accounts for the change in the distribution function due to inter-particle collisions. For smooth inelastic spheres is of the form,

$$\frac{\partial_{\mathrm{c}}(nf)}{\partial t} = n^2 \chi\left(n, \left(\mathbf{x}+\mathbf{x}^*/2\right)\right) \int \mathrm{d}\mathbf{a} \int \mathrm{d}\mathbf{u}^* \left(e_{\mathrm{n}}^{-2} f\left(\mathbf{x},\mathbf{u}'\right) f\left(\mathbf{x}^*,\mathbf{u}^{*'}\right) - f(\mathbf{x},\mathbf{u}) f\left(\mathbf{x}^{*'},\mathbf{u}^*\right)\right) \mathbf{w}\cdot\mathbf{a} d^2 \tag{5}$$

where d is the particle diameter, $(\mathbf{x},\mathbf{u})$ and $(\mathbf{x}^*,\mathbf{u}^*)$ are the positions and velocities of the colliding particles in a 'forward' collision that results in a depletion of particles in the differential volume $\mathrm{d}\mathbf{x}\mathrm{d}\mathbf{u}$, and $(\mathbf{x},\mathbf{u}')$ and $(\mathbf{x}^{*'},\mathbf{u}^{*'})$ are the velocities of particles in an 'inverse' collision that results in an accumulation of particles in the differential volume $\mathrm{d}\mathbf{x}\mathrm{d}\mathbf{u}$. The factor of e_{n}^{-2} in the accumulation term, which is not present in the kinetic theory of gases, accounts for the change in the magnitude of the relative velocity $(\mathbf{w}\cdot\mathbf{n})$ in an inelastic collision, and the contraction in the phase space differential volume energy dissipation. The term $(\chi(n,(\mathbf{x}+\mathbf{x}^*)/2))$ is the 'pair distribution function' at the point of contact between the two particles, $(\mathbf{x}+\mathbf{x}^*)/2$. In the dilute limit, the finite volume of the particles is neglected and we set $\mathbf{x}^* = \mathbf{x}$ in the collision integral, and the pair distribution function is 1, to obtain the Boltzmann equation. As the volume fraction increases, the pair distribution function accounts for the 'excluded volume' effect (the entire fluid volume is not available to a test particle, because some of the volume is occupied by other particles) and the 'shadowing effect' (two particles cannot collide if there is a third particle in between these). An accurate description of the pair distribution function is essential for modelling dense granular flows. It should be noted that in the collision integral (5), the molecular chaos approximation has been used in the dilute limit where the two-particle distribution function is written as the product of the single-particle distribution function, and the Enskog approximation has been used for dense gases, where the two-particle distribution function is written as the product of the single-particle distributions and the pair distribution function at contact.

Conservation equations are derived by multiplying the Boltzmann equation (conservation equation for the distribution function) by mass, momentum and energy, and integrating over the velocity co-ordinates. If we multiply by particle mass and integrate over the fluctuating velocity $\mathbf{c}$, we obtain:

$$\frac{\mathrm{d}\rho}{\mathrm{d}t} + \rho\frac{\partial U_j}{\partial x_j} = 0 \tag{6}$$

where $(\mathrm{d}/\mathrm{d}t)$ is the substantial derivative.

Multiplying by mu_i, and noting that the average of the fluctuating velocity is zero, we obtain:

$$\rho\frac{\mathrm{d}U_i}{\mathrm{d}t} = \frac{\partial\sigma_{ij}}{\partial x_j} + \rho a_i \tag{7}$$

The energy balance equation is obtained by multiplying the Boltzmann equation by $(mc_i^2/2)$ and integrating over the particle velocities. In the energy balance equation, the specific energy (per unit mass) is expressed in terms of the 'granular temperature' using $e = C_v T$, where C_v is the specific heat at constant volume. The energy balance equation is of the form,

$$nC_v\frac{\mathrm{d}T}{\mathrm{d}t} = -\frac{\partial q_j}{\partial x_j} + \sigma_{ij}\frac{\partial U_i}{\partial x_j} - D \tag{8}$$

These are the mass, momentum and energy conservation equations. The constitutive relations are then determined by calculating the fluxes of mass, momentum and energy generated by the corrections to the distribution function [29] due to applied velocity or temperature gradients. The resulting constitutive relations for the stress, the heat flux and the dissipation coefficient are of the form

$$\sigma_{ij} = -p + \mu(e_\mathrm{n}, e_\mathrm{t})\left(\frac{\partial U_i}{\partial x_j} + \frac{\partial U_j}{\partial x_i} - \frac{2\delta_{ij}}{3}\frac{\partial U_k}{\partial x_k}\right) + \mu_\mathrm{b}(e_\mathrm{n}, e_\mathrm{t})\delta_{ij}\frac{\partial U_k}{\partial x_k} \tag{9}$$

$$q_i = -K(e_\mathrm{n}, e_\mathrm{t})\frac{\partial T}{\partial x_i} - \alpha(e_\mathrm{n}, e_\mathrm{t})\frac{\partial n}{\partial x_i} \tag{10}$$

$$D = -\rho C_v\xi(e_\mathrm{n}, e_\mathrm{t})T^{3/2} \tag{11}$$

where p is the pressure, μ and μ_b are the shear and bulk viscosity, K is the thermal conductivity, and α is the thermal diffusion coefficient, indicial notation is used to represent vectors and a repeated index denotes a dot product. The coefficients $\alpha(e_\mathrm{n}, e_\mathrm{t})$ and $\xi(e_\mathrm{n}, e_\mathrm{t})$ are zero for rough elastic particles with $(e_\mathrm{n} = 1, e_\mathrm{t} = -1)$ or for smooth elastic particles with $(e_\mathrm{n} = 1, e_\mathrm{t} = 1)$. and are non-zero only for $e_\mathrm{n} < 1$ and/or $|e_\mathrm{t}| < 1$. The bulk viscosity μ_b is zero for an elastic fluid in the dilute limit, but is non-zero at moderate and high densities where collisional contributions to the stress become important.

In the constitutive relations, the fluxes across a virtual surface in the fluid can be classified into two categories. The kinetic flux is due to the physical transport of a particle across the surface that carries along its mass, momentum or energy. The collisional flux is due to the collision of a particle with centre on one side of the surface with another particle on the other side, which results in a transport of momentum or energy. The kinetic flux is dominant in the dilute limit, but as the system becomes denser, the collisional flux dominates because the frequency of particle transport across the surface is hindered by the presence of neighbouring particles. The collisional flux depends on the pair distribution function at contact χ used in the collision integral [29], where $n\chi$ is the number of particles that are in contact with a test particle. The pair distribution function is 1 in the dilute limit, but is larger than 1 for dense particle assemblies due to the excluded volume and screening effects [29]. It is necessary to accurately model the pair distribution function in dense granular flows in order to predict the flow dynamics.

The forms of the transport coefficients can be deduced on the basis of dimensional analysis for a hard-particle system. The dimensional parameters are the mass m and diameter d of the particles, and the dimensionless parameters are the volume fraction and the coefficients of restitution and friction. As there is no material time scale or energy scale in a hard-particle system, the time scale has to be obtained by a suitable combination of (T/m) (with dimensions of the square of the velocity) and the particle mass and diameter. On this basis, the forms of the pressure, viscosity, thermal conductivity and energy dissipation rate are,

$$\begin{aligned}
p &= p'\left(T/d^3\right)\\
\mu &= \mu'\left((mT)^{1/2}/d^2\right)\\
\mu_\mathrm{b} &= \mu'_\mathrm{b}\left((mT)^{1/2}/d^2\right)\\
K &= K'\left((T/m)^{1/2}/d^2\right)\\
\alpha &= \alpha'\left((T/m)^{1/2}Td\right)\\
D &= D'\left(T(T/m)^{1/2}/d^4\right)
\end{aligned} \tag{12}$$

where p', μ', μ'_b, K', α' and ξ' are dimensionless functions of the volume fraction and coefficients of restitution, and α' and D' are proportional to $(1 - e^2)$ for nearly elastic particles with coefficient of restitution close to 1. The forms of the transport coefficients can be specified more narrowly in for dilute and dense granular flows. In the dilute limit, the relevant length scale is not the particle diameter, but the mean free path that is the distance between successive collisions, and is

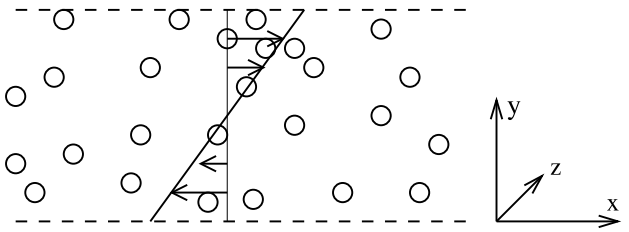

Fig. 3. A linear shear flow with velocity in the x direction, and velocity gradient in the y direction.

proportional to $(nd^2)^{-1}$, where n is the number density and d is the particle diameter. In this case, the expressions for the transport coefficients are of the form,

$$\begin{aligned} p &= p^{\dagger} nT \\ \mu &= \mu^{\dagger}\left((mT)^{1/2}/d^2\right) \\ \mu_{\mathrm{b}} &= \mu_{\mathrm{b}}^{\dagger}\left((mT)^{1/2}/d^2\right) \\ K &= K^{\dagger}\left((T/m)^{1/2}/d^2\right) \\ \alpha &= \alpha^{\dagger}\left((T/m)^{1/2}Td\right) \\ \xi &= D^{\dagger}\left(n^2d^2T(T/m)^{1/2}\right) \end{aligned} \tag{13}$$

where $p^{\dagger}$, $\mu^{\dagger}$, $\mu_{\mathrm{b}}^{\dagger}$, $K^{\dagger}$, $\alpha^{\dagger}$ and $D^{\dagger}$ are dimensionless functions of the coefficient of restitution. For a dense flow, transport is predominantly collisional, and all of the transport coefficients are proportional to the pair distribution function $\chi(\phi)$, which is large. In this case, the transport coefficients are of the form given in Eq. (12), where p', μ', μ_{b}', K', α' and D' are equal to the pair distribution function χ times a function of the coefficients of restitution.

Constitutive relations of the form given in Eqs. (9) and (10) have been derived using the Chapman–Enskog procedure, or a procedure based on Grad's moments for the velocity distributions where balance equations are written for a specified sub-set of the moments of the velocity distribution. The earlier calculations [30–34] focused on the terms that are linear in the temperature and velocity gradients, and have derived constitutive relations similar to Eq. (12). There have been subsequent calculations [35–37,25,26,38] that have calculated parts of the next higher 'Burnett' corrections, which are second order in the velocity and temperature gradients not included in Eq. (9). These terms are difficult to calculate, but they could give rise to important effects such as the normal stress differences that are observed in real granular flows.

In a linear shear flow, where the flow is in the x direction and the velocity gradient in the y direction, as shown in Fig. 3, the energy equation is of the form

$$\mu\left(\frac{\partial u_x}{\partial y}\right)^2 = D \tag{14}$$

where the left side of the equation represents the source of energy due to mean shear, and the right side is the rate of dissipation of energy. For a dilute sheared granular flow, Eq. (13) indicates that the viscosity is proportional to $(T^{1/2}/d^2)$, while the rate of dissipation of energy is proportional to $n^2d^2T^{3/2}(1-e^2)$. Therefore, the energy balance equation provides a relation between the strain rate and the temperature:

$$\frac{\partial u_x}{\partial y} \propto \left(1-e^2\right)^{1/2}(T/m)^{1/2}nd^2 \tag{15}$$

Therefore, the mean strain rate is proportional to $(1-e^2)^{1/2}$ times the root mean square fluctuating velocity divided by the mean free path $(nd^2)^{-1}$. For nearly elastic particles with $(1-e^2) \ll 1$, an expansion can be used in the small parameter $\epsilon = (1-e^2)^{1/2}$. When the Boltzmann equation is expanded in the parameter ϵ, the elastic Boltzmann equation is the $O(1)$ approximation, and the solution to this equation is the Maxwell–Boltzmann distribution. However, the temperature is not specified by thermodynamic considerations, but rather by a balance between the production and dissipation of energy that appear at $O(\epsilon^2)$ in the expansion.

The objective of many of the pioneering granular kinetic theory studies [30–32] was the derivation of constitutive relations for sheared granular flows. These were then inserted into the mass, momentum and energy conservation equations to obtain solutions for the density, mean velocity and temperature. More recent studies have made a distinction between the mass and momentum equations, which are written for conserved variables, and the energy equation since energy is not a conserved variable in a granular flow. A local input of energy can be dissipated due to collisions, and it does not have to be conducted undiminished as required for a system with elastic collisions. The non-conserved nature of the energy

also introduces an additional length scale in the flow, the conduction length, which is the distance to which an energy input is conducted before its magnitude diminishes due to dissipation. This conduction length can be estimated as follows [25,26,39,40].

From the transport and dissipation coefficients in Eq. (13), the divergence of the energy flux is proportional to $(KT/L^2) \sim K^\dagger((T/m)^{1/2}(T/L^2d^2))$, where L is the length scale for the temperature variations. The rate of dissipation of energy is proportional to $D^\dagger n^2 d^2 T(T/m)^{1/2}$. Comparing the two, we see that the rate of conduction of energy is much smaller (larger) than the rate of dissipation of energy for $L \gg L_c$ ($L \ll L_c$), where the conduction length $L_c = (nd^2)^{-1}(1-e^2)^{-1/2}$, the ratio of the mean free path and $(1-e^2)^{1/2}$. For nearly elastic particles, the conduction length is $(1-e^2)^{-1/2}$ larger than the mean free path, while the conduction length and mean free path are comparable for highly inelastic particles when the coefficient of restitution is not close to 1. For dense granular flows, the microscopic length scale is the particle diameter and not the mean free path, and so the conduction length can be estimated as $(d/(1-e^2)^{1/2})$, in the nearly elastic limit. If the flow length scale is smaller than the conduction length, then energy is conducted throughout the flow domain before it is significantly dissipated by inelastic collisions, and energy can be considered a conserved variable. If the flow length scale is much larger than the conduction length, any input of energy is dissipated locally over a length scale small compared to the macroscopic scale. The energy equation reduces to an algebraic balance between the source of energy due to mean shear and the dissipation due to inelastic collisions, and the temperature is determined from this local balance. There are regions near the boundaries where the energy conduction is important over length scales comparable to the conduction length, and these have been treated using boundary layer theory [39].

A more detailed rheological description that includes normal stress differences, as well as tracer diffusion coefficients, for sheared granular flows have been calculated using the Chapman–Enskog procedure [26], as well as by the Grad's moment expansions [41–44]. The results are in very good agreement with simulation results based on the Direct Simulation Monte Carlo procedure even at high dissipation. Non-linear transport coefficients [45,46] have been calculated for momentum and heat transport around the uniform sheared state, and these are found to be different from those in the Navier–Stokes equations. The other non-conserved variable that has been used in macroscopic descriptions is the average of the particle angular velocity. Kinetic theory for rough particles predicts that the particle angular velocity has to be equal to one half of the local vorticity in the bulk of the flow. However, there could be regions near boundaries where the angular velocity is not equal to one half of the vorticity, due to spin induced by the particle interaction with the boundaries [47]. The thicknesses of these regions is comparable to the mean free path for dilute flows, and the particle diameter for dense flows in the case of rough particles, though it could be larger for particles that are nearly smooth. In these regions, the stress tensor is not symmetric, and there is an antisymmetric component of the stress tensor proportional to the difference between the average angular velocity of the particles and one half of the local vorticity. In addition to the mass and momentum equations, there is the requirement of an additional equation for the particle spin.

The stability of the uniform sheared state of a granular flow has been of much interest since the pioneering studies of Savage [48], Babic [49] and Schmid and Kytomaa [50]. These first studies were motivated by the observation that in simulation of sheared granular flows, the granular temperature is higher than that predicted by kinetic theory, suggesting that the 'laminar' state of the flow is unstable and the flow has undergone a transition to a 'turbulent' state with enhanced velocity fluctuations. Several linear stability studies have been performed both of a simple shear flow [51,25], as well as for more complicated flows such as the flow down an inclined plane [52–54], and non-linear stability studies of granular flows in order to determine the nature of the bifurcation [55,56]. The stability analysis for a homogeneous shear flow is a little different from the usual linear stability analysis for fluid systems, because the wave vector is usually considered to be time dependent, and rotating with the mean shear, in order to obtain an eigenvalue problem. Due to the rotation with the mean shear, the wave vector with initial orientation in the flow plane is aligned, at long times, in the gradient direction. Though perturbations that have a component of the wave vector in the flow direction may be transiently unstable, they are rotated and aligned with the gradient direction in the long time limit, and so the flow stability is dependent on the alignment of perturbations with wave vector in the gradient direction, or in the span wise direction perpendicular to the flow plane. The broad conclusion of the linear stability studies is that the flows are unstable to the layering instability, where layers form with modulation in the gradient direction or in the spanwise direction, but the most unstable modes have sufficiently long wavelength that they may not be observed in simulations of small size.

In the linear stability studies, the coefficients in Eq. (12) are assumed to have specific dependences on the volume fraction and the coefficient of restitution. These forms are usually chosen on the basis of simulation results for hard sphere fluids, or based on kinetic theory calculations in the Enskog approximation. The forms of these functions are sometimes altered in order to fit simulation results for inelastic sphere configurations. This is not completely satisfactory in the dense limit, since the stability depends on the forms of the functions used in the constitutive relations. Moreover, in the dense limit, the pair distribution functions increases sharply for small changes in the volume fraction, and the results become sensitive to the form of the divergence of the pair distribution function.

It is necessary to carefully specify the meaning of the term 'kinetic theory', which is often used in two different contexts. The first is a general mesoscopic approach, where the state of the system is described using the distribution function that specifies the distribution of particle positions and velocities. This approach is general, but not possible to solve exactly in most cases. The second context is to the approximations such as the molecular chaos approximation in the Boltzmann or Enskog approximation in Eq. (4), where the two particle distribution is expressed as the product of the single particle velocity distribution functions and the pair distribution function at contact. This is an uncontrolled approximation in the dense

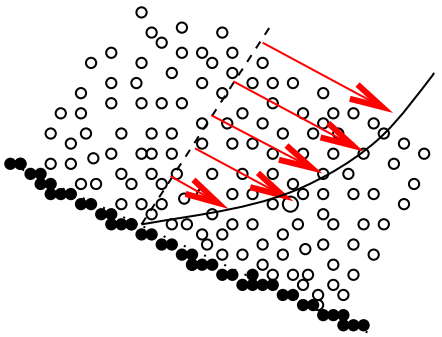

Fig. 4. (Colour online.) Dense granular flow down an inclined plane on a rough base.

limit, since there is no small parameter (unlike the dilute limit where the density can be considered a small parameter). When the results of the theory are not in agreement with experimental/simulation results, this is often due to the failure of the approximate models where the correlations are neglected, rather than the general mesoscopic approach. A systematic improvement of the models to incorporate the effect of correlations, within the context of the same mesoscopic approach, is necessary to accurately describe granular flows in the dense flow regime. Here, the general mesoscopic approach is referred to as 'kinetic theory', and we discuss, in the next section, how the approximate models can be improved to incorporate the effect of correlations in dense flows.

4. Dense granular flows

Interest in kinetic theories for dense granular flows was stimulated by pioneering particle-level simulation studies [15–17] and experiments [57] on the dense granular flow down an inclined plane, Fig. 4, which revealed several interesting and unusual features. In simulations using the spring-dashpot model, the flow usually starts when the angle of inclination exceeds about 21°, and a stable flow regime is observed up to an inclination angle of about 25°. In the bulk of the flow excluding 3–5 particle layers at the base and the free surface, the volume fraction is found to be independent of depth, contrary to the expectation that the volume fraction should increase with flow depth due to the increased over-burden. The velocity profile satisfies Bagnold's law even at high volume fractions in the range 55–59%, strongly suggesting that the interactions could be modelled as instantaneous binary collisions. However, constitutive relations based on kinetic theory were not able to predict flow properties—for example, as the angle of inclination increases, the volume fraction is predicted to increase and the system becomes more dense. The reasons for the wrong predictions were traced to [39,58,59].

1. The accuracy of the pair distribution function at contact, χ.
2. The molecular chaos approximation for a dilute flow, and the Enskog approximation for dense flows where the two-particle distribution at contact is written as the product of the spatial pair distribution function and their single-particle velocity distributions.

In a dense granular flow, the transport of momentum and energy occurs primarily due to collisions, and accurate modelling of the pair distribution function is essential for capturing the flow dynamics. The most widely used form of the pair distribution function for moderate volume fractions (up to about 0.4) is the 'Carnahan–Starling' [60] pair distribution function, which in three dimensions is:

$$\chi(\phi) = \frac{2-\phi}{2(1-\phi)^3} \tag{16}$$

This pair distribution function is applicable for moderate volume fractions, but it diverges at a volume fraction of 1. This is clearly unphysical, since in a real collection of spherical particles, the volume fraction can never reach 1.

Hard disk and hard sphere system exhibit a transition upon the change in the volume fraction, rather than the temperature. In three dimensions, for example, there is a freezing transition at a volume fraction of 0.494, where the system transitions from a random state to a crystal state. Even though there is a crystallisation transition, the system can be maintained in the random state even at high volume fractions by fast compression or 'quenching'. In simulations, this is carried out by swelling the particles until two touch, and then carrying out a random (Monte Carlo) move. The random quenched state becomes 'jammed' at a volume fraction called the 'random close packing' (RCP) volume fraction $\phi_c \approx 0.64$, beyond which it cannot be compressed further. For a hard sphere system in the random state, a pair distribution function has been suggested by Torquato [61], which diverges at the random close-packing volume fraction,

$$\chi(\phi) = \frac{(2-\phi_f)}{2(1-\phi_f)^3}\frac{(\phi_c-\phi_f)}{(\phi_c-\phi)} \tag{17}$$

where, $\phi_c = 0.64$ is the volume fraction at random close packing, $\phi_f = 0.49$ is the volume fraction at freezing. This smoothly makes a transition from the Carnahan–Starling pair distribution function to one that diverges as $(\phi_c - \phi)^{-1}$ as the random close packing volume fraction is approached.

A hard-sphere sheared inelastic fluid can be treated in a manner similar to an elastic hard-sphere fluid, with the stipulation that the strain rate and the granular temperature are coupled through the energy balance condition. Simulations of a sheared inelastic hard-particle fluid show that the crystallisation transition is suppressed by shear [58,59], since it is not possible to shear a crystal with hexagonal close packing or face centred cubic order in a manner that does not disrupt ordering. Due to this, the maximum attainable volume fraction for a sheared inelastic hard sphere fluid is about 0.59. This is the reason for shear dilation in sheared granular flow—whereas the volume fraction can be as high as 0.64 in the static state, a sheared granular flow has a maximum volume fraction of about 0.59, and so the material has to dilate in order to accommodate shear. For this reason, studies on dense granular flows down an inclined plane [62,63] have modified the pair distribution function [61] and used $\phi_c = 0.6$.

It has been recognised for some time now [16] that the kinetic theory predictions for the energy dissipation rate in the dense limit is higher than that observed in simulations of dense granular flows. While earlier studies [62,63] have attributed this to the formation of clusters in a dense granular flow, later studies [58,59] indicated that the dissipation rate is strongly affected by a correlation in the distribution of relative velocities of pairs of colliding particles [58,59]. In an elastic fluid at equilibrium, equipartition requires a factorisation of the two-particle velocity distribution function into two Maxwell–Boltzmann distributions with equal temperature. In a driven dissipative system, there is no such requirement, and simulation studies [59] have shown that the two-particle relative velocity distribution function transitions from a Maxwell–Boltzmann distribution for nearly elastic particles to an exponential distribution for inelastic particles. Even when the relative velocity distribution is exponential, it was found that the single particle distribution is close to a Maxwell–Boltzmann distribution, and the variance of the relative velocity distribution is much smaller than that for the single-particle distribution. Due to the change in the form of the relative velocity distribution, there is a reduction in the stress and energy dissipation. However, the fractional reduction in the energy dissipation rate (related to the third moment of the velocity distribution) is larger than that in the stress (related to the second moment of the velocity distribution). It was found that when the relative velocity distribution is used in kinetic theory calculations, the correct stress and dissipation rates are predicted [58,59].

One of the successes of kinetic theory is that all the salient features of the dense granular flow down an inclined plane, including the presence of 'conduction' boundary layers at the top and bottom surfaces, the cessation of flow at a non-zero angle of inclination, the normal stress differences and the dependence of the height for cessation of flow on the angle of inclination [57] are well predicted when sufficient detail is included in the kinetic theory [39,58,59]. However, it is necessary to add in the effect of correlations in the velocity distribution from simulations in order to be able to make accurate predictions. The important outstanding challenge is to derive, from first principles, the effect of correlations on the relative velocity distributions in a dense granular flow, in order to set up a comprehensive theoretical framework.

Acknowledgements

The author would like to thank the Department of Science and Technology, Ministry of Science and Technology, Government of India for financial support. The author would like to thank V. Garzo and J.W. Dufty for their valuable comments.

References

[1] M. Faraday, On a peculiar class of acoustical figures; and on certain forms assumed by groups of particles upon vibrating elastic surfaces, Philos. Trans. R. Soc. Lond. 52 (1831) 299–340.
[2] K. Kumar, E. Falcon, K.M.S. Bajaj, S. Fauve, Shape of convective cell in Faraday experiment with fine granular materials, Physica A 270 (1999) 97–104.
[3] H.K. Pak, R.P. Behringer, Surface waves in vertically vibrated granular materials, Phys. Rev. Lett. 71 (1993) 1832–1835.
[4] P.B. Umbanhowar, F. Melo, H.L. Swinney, Localized excitations in a vertically vibrated granular layer, Nature 382 (1996) 793–796.
[5] J. Bougie, J. Kreft, J.B. Swift, H.L. Swinney, Onset of patterns in an oscillated granular layer: continuum and molecular dynamics simulations, Phys. Rev. E 71 (2005) 021301.
[6] P. Sunthar, V. Kumaran, Characterization of the stationary states of a dilute vibrofluidized granular bed, Phys. Rev. E 64 (2001) 041303.
[7] R. Ramírez, D. Risso, P. Cordero, Thermal convection in fluidized granular systems, Phys. Rev. Lett. 85 (2000) 1230–1233.
[8] R. Bagnold, Experiments on a gravity-free dispersion of large solid spheres in a Newtonian fluid under shear, Proc. R. Soc. Lond. A 225 (1954) 49–63.
[9] R. Bagnold, The flow of cohesionless grains in fluids, Proc. R. Soc. Lond. A 249 (1954) 235–297.
[10] M.L. Hunt, R. Zenit, C.S. Campbell, C.E. Brennen, Revisiting the 1954 suspension experiments of R.A. Bagnold, J. Fluid Mech. 452 (2002) 1–24.
[11] P.A. Cundall, O.D.L. Strack, A discrete numerical model for granular assemblies, Geotechnique 29 (1979) 47–65.
[12] O.R. Walton, Numerical simulation of inclined chute flows of monodisperse, inelastic, frictional spheres, Mech. Mater. 16 (1993) 239–247.
[13] C.S. Campbell, Granular shear flows at the elastic limit, J. Fluid Mech. 465 (2002) 261.
[14] C.S. Campbell, Stress-controlled elastic granular shear flows, J. Fluid Mech. 539 (2005) 273.
[15] L.E. Silbert, D. Ertas, G.S. Grest, T.C. Halsey, D. Levine, S.J. Plimpton, Granular flow down an inclined plane: Bagnold scaling and rheology, Phys. Rev. E 64 (2001) 051302.
[16] Namiko Mitarai, Hiizu Nakanishi, Bagnold scaling, density plateau, and kinetic theory analysis of dense granular flow, Phys. Rev. Lett. 94 (Apr 2005) 128001.
[17] K.A. Reddy, V. Kumaran, Applicability of constitutive relations from kinetic theory for dense granular flows, Phys. Rev. E 76 (2007) 061305.
[18] K.A. Reddy, V. Kumaran, Dense granular flow down an inclined plane: a comparison between the hard particle model and soft particle simulations, Phys. Fluids 22 (2010) 113302.
[19] R.D. Mindlin, H. Deresiewicz, Elastic spheres in contact under varying oblique forces, J. Appl. Mech. 20 (1953) 327–344.

[20] D.M. Cole, J.F. Peters, A physically based approach to granular media mechanics: grain-scale experiments, initial results and implications to numerical modelling, Granul. Matter 9 (2007) 309–321.
[21] D.M. Cole, J.F. Peters, Grain-scale mechanics of geologic materials and lunar simulants under normal loading, Granul. Matter 10 (2008) 171–185.
[22] F.B. Pidduck, The kinetic theory of a special type of rigid molecule, Proc. R. Soc. A, Math. Phys. Eng. Sci. 101 (1922) 101–112.
[23] G.H. Bryan, Report on the present state of our knowledge of thermodynamics, Brit. Assoc. Rep. 64 (1894) 62–102.
[24] S.F. Foerster, M.Y. Louge, H. Chang, K. Allia, Measurements of the collision properties of small spheres, Phys. Fluids 6 (1994) 1108–1115.
[25] V. Kumaran, Constitutive relations and linear stability of a sheared granular flow, J. Fluid Mech. 506 (2004) 1–42.
[26] V. Kumaran, The constitutive relation for the granular flow of rough particles, and its application to the flow down an inclined plane, J. Fluid Mech. 561 (2006) 1–42.
[27] Gilberto M. Kremer, Andrés Santos, Vicente Garzó, Transport coefficients of a granular gas of inelastic rough hard spheres, Phys. Rev. E 90 (Aug 2014) 022205.
[28] C. Campbell, Clusters in dense-inertial granular flows, J. Fluid Mech. 687 (2011) 341–359.
[29] S. Chapman, T.G. Cowling, The Mathematical Theory of Non-Uniform Gases, Cambridge Mathematical Library, 1991.
[30] S.B. Savage, D.J. Jeffrey, The stress tensor in a granular flow at high shear rates, J. Fluid Mech. 110 (1981) 255–272.
[31] J.T. Jenkins, M.W. Richman, Grad's 13-moment system for a dense gas of inelastic spheres, Arch. Ration. Mech. Anal. 87 (1985) 355–377.
[32] C.K.K. Lun, S.B. Savage, D.J. Jeffrey, N. Chepurniy, Kinetic theories for granular flow: inelastic particles in couette flow and slightly inelastic particles in a general flowfield, J. Fluid Mech. 140 (1984) 223–256.
[33] C.K.K. Lun, Kinetic theory for the flow of dense, slightly inelastic, slightly rough spheres, J. Fluid Mech. 233 (1991) 539–559.
[34] V. Garzo, J.W. Dufty, Dense fluid transport for inelastic hard spheres, Phys. Rev. E 59 (May 1999) 5895–5911.
[35] N. Sela, I. Goldhirsch, S.H. Noskowicz, Kinetic theoretical study of a simply sheared two dimensional granular gas to Burnett order, Phys. Fluids 8 (1996) 2337–2353.
[36] N. Sela, I. Goldhirsch, Hydrodynamic equations for rapid flows of smooth inelastic spheres, to Burnett order, J. Fluid Mech. 361 (1998) 41–74.
[37] I. Goldhirsch, N. Sela, Origin of normal stress differences in rapid granular flows, Phys. Rev. E 54 (Oct 1996) 4458–4461.
[38] Nagi Khalil, Vicente Garzó, Andrés Santos, Hydrodynamic Burnett equations for inelastic maxwell models of granular gases, Phys. Rev. E 89 (May 2014) 052201.
[39] V. Kumaran, Dense granular flow down an inclined plane: from kinetic theory to granular dynamics, J. Fluid Mech. 599 (2008) 121–168.
[40] V. Kumaran, Dynamics of a dilute sheared inelastic fluid, I: hydrodynamic modes and velocity correlation functions, Phys. Rev. E 79 (2009) 011301.
[41] Andrés Santos, Vicente Garzó, James W. Dufty, Inherent rheology of a granular fluid in uniform shear flow, Phys. Rev. E 69 (Jun 2004) 061303.
[42] J.M. Montanero, V. Garzo, Rheological properties in a low-density granular mixture, Physica A 310 (2002) 17–38.
[43] Garzó Vicente, Tracer diffusion in granular shear flows, Phys. Rev. E 66 (Aug 2002) 021308.
[44] James F. Lutsko, Rheology of dense polydisperse granular fluids under shear, Phys. Rev. E 70 (Dec 2004) 061101.
[45] Garzó Vicente, Transport coefficients for an inelastic gas around uniform shear flow: linear stability analysis, Phys. Rev. E 73 (Feb 2006) 021304.
[46] James F. Lutsko, Chapman–Enskog expansion about nonequilibrium states with application to the sheared granular fluid, Phys. Rev. E 73 (Feb 2006) 021302.
[47] Namiko Mitarai, Hisao Hayakawa, Hiizu Nakanishi, Collisional granular flow as a micropolar fluid, Phys. Rev. Lett. 88 (Apr 2002) 174301.
[48] S.B. Savage, Instability of unbounded uniform granular shear flow, J. Fluid Mech. 241 (1992) 109–123.
[49] M. Babic, On the stability of rapid granular flows, J. Fluid Mech. 254 (1993) 127–158.
[50] P.J. Schmid, H.K. Kytomaa, Transient and asymptotic stability of granular shear flow, J. Fluid Mech. 264 (1994) 255–275.
[51] M. Alam, P.R. Nott, Stability of plane couette flow of a granular material, J. Fluid Mech. 377 (1999) 99–136.
[52] N. Mitarai, H. Nakanishi, Linear stability analysis of rapid granular flow down a slope and density wave formation, J. Fluid Mech. 507 (2004) 309–334.
[53] Y. Forterre, O. Pouliquen, Stability analysis of rapid granular chute flows: formation of longitudinal vortices, J. Fluid Mech. 467 (2002) 361–387.
[54] M.J. Woodhouse, A.J. Hogg, Rapid granular flows down inclined planar chutes, Part 2: linear stability analysis of steady flow solutions, J. Fluid Mech. (2010) 461–488.
[55] P. Shukla, M. Alam, Nonlinear stability and patterns in granular plane couette flow: Hopf and Pitchfork bifurcations, and evidence for resonance, J. Fluid Mech. 672 (2011) 147–195.
[56] P. Shukla, M. Alam, Nonlinear vorticity-banding instability in granular plane couette flow: higher-order landau coefficients, bistability and the bifurcation scenario, J. Fluid Mech. 718 (2013) 131–180.
[57] O. Pouliquen, Scaling laws in granular flows down rough inclined planes, Phys. Fluids 11 (1999) 542–548.
[58] V. Kumaran, Dynamics of dense sheared granular flows, Part I: structure and diffusion, J. Fluid Mech. 632 (2009) 109–144.
[59] V. Kumaran, Dynamics of dense sheared granular flows, Part II: the relative velocity distribution, J. Fluid Mech. 632 (2009) 109–145.
[60] N.F. Carnahan, K.E. Starling, Equation of state for nonattracting rigid spheres, J. Chem. Phys. 51 (1969) 635–636.
[61] S. Torquato, Nearest-neighbor statistics for packings of hard spheres and disks, Phys. Rev. E 51 (Apr 1995) 3170–3182.
[62] J.T. Jenkins, Dense shearing flows of inelastic disks, Phys. Fluids 18 (2006) 103307.
[63] J.T. Jenkins, Dense inclined flows of inelastic spheres, Granul. Matter 10 (2007) 47–52.